Vesicle Permeabilization by Protofibrillar α-Synuclein Is Sensitive to Parkinson's Disease-Linked Mutations and Occurs by a Pore-like Mechanism†

Michael J. Volles and Peter T. Lansbury, Jr.*

Center for Neurologic Diseases, Brigham and Women's Hospital, and Department of Neurology, Harvard Medical School, 65 Landsdowne Street, Cambridge, Massachusetts 02139

Received December 10, 2001; Revised Manuscript Received January 29, 2002

ABSTRACT: Two mutations in the protein α-synuclein (A30P and A53T) are linked to an autosomal dominant form of Parkinson's disease. Both mutations accelerate the formation of prefibrillar oligomers (protofibrils) in vitro, but the mechanism by which they promote toxicity is unknown. Protofibrils of wild-type α-synuclein bind and permeabilize acidic phospholipid vesicles. This study examines the relative membrane permeabilizing activities of the wild type, mutant, and mouse variants of protofibrillar α-synuclein and the mechanism of membrane permeabilization. Protofibrillar A30P, A53T, and mouse variants were each found to have greater permeabilizing activities per mole than the wild-type protein. The leakage of vesicular contents induced by protofibrillar α-synuclein exhibits a strong preference for low-molecular mass molecules, suggesting a pore-like mechanism for permeabilization. Under conditions in which the vesicular membrane is less stable (lack of calcium as a phospholipid counterion), protofibril permeabilization is less size-selective and monomeric α-synuclein can permeabilize via a detergent-like mechanism. We conclude that the pathogenesis of Parkinson's disease may involve membrane permeabilization by protofibrillar α-synuclein, the extent of which will be strongly dependent on the in vivo conditions.

The clinical features of Parkinson's disease (PD)[1] are caused by degeneration of dopaminergic neurons in the *substantia nigra*. This degeneration is concomitant with the formation of Lewy bodies (LBs), intracellular inclusions composed predominantly of fibrillar α-synuclein (*1*). Two point mutations in α-synuclein [A30P (*2*) and A53T (*3*)], a natively unfolded protein (*4*) of unknown function, are linked to rare forms of autosomal-dominant PD.

Monomeric α-synuclein aggregates in vitro via a metastable oligomeric (protofibril) state, and on to stable fibrils, at which time protofibrils are consumed (*5*). Several differences in the aggregation behavior of the PD-linked mutants and the wt protein have been observed. The protofibrillization rate of both mutants is increased relative to that of wt (*5*, *6*), but the fibrillization rate is decreased in one case (A30P) and increased in the other (A53T) (*5*−*8*). The mouse homologue of α-synuclein fibrillizes faster than either of the mutants or the wt protein, while mixtures of wt and mouse proteins show a kinetic stabilization of protofibrillar α-synuclein resulting in a decreased rate of fibril formation (*9*). Interestingly, a human α-synuclein transgenic mouse model of PD (*10*), which expresses both human and mouse forms of α-synuclein, does not produce fibrillar α-synuclein but does exhibit neurodegeneration, motor dysfunction, and nonfibrillar inclusions. In addition, dopamine adducts of α-synuclein prolong the lifetime of protofibrillar species while inhibiting fibril formation (*11*). These data, taken together, suggest that a protofibrillar species, other than the fibril, may be a toxic entity in PD. The potential mechanism of toxicity of protofibrillar α-synuclein is not known, and we searched for candidate mechanisms by looking for properties that distinguished the monomeric and protofibrillar forms.

Monomeric α-synuclein binds negatively charged phospholipid membranes and, in so doing, undergoes a structural transition to α-helix (*12*−*16*). The A30P mutant is less effective in binding (*13*, *17*), probably because of disruption of N-terminal helical structure by the additional proline (*18*). Protofibrillar α-synuclein (wt) binds negatively charged lipids more strongly than the monomer (*12*). Permeabilization of negatively charged vesicles to calcium is induced by the protofibrillar but not the monomeric or fibrillar forms of wt α-synuclein (*12*). Finally, annular α-synuclein protofibril structures which are reminiscent of the known structures of naturally occurring toxin pores (*19*) have been observed by AFM (*5*; T. Ding and P. T. Lansbury, Jr., unpublished) and EM (H. Lashuel and P. T. Lansbury, Jr., unpublished). These data led us to propose membrane permeabilization by protofibrillar α-synuclein as a toxic mechanism consistent with our understanding of PD pathogenesis (*12*).

† This work was supported by an NINDS Morris K. Udall Parkinson's Disease Research Center of Excellence Grant (NS38375) and the NIA (AG14366). M.J.V. was supported by a predoctoral fellowship from the National Science Foundation.

* To whom all correspondence should be addressed. Telephone: (617) 768-8610. Fax: (617) 768-8606. E-mail: plansbury@rics.bwh.harvard.edu.

[1] Abbreviations: AFM, atomic force microscopy; cytC, cytochrome *c*; DOPA, 1,2-dioleoyl-*sn*-glycero-3-phosphate; DOPG, 1,2-dioleoyl-*sn*-glycero-3-[phospho-*rac*-(1-glycerol)]; DOPS, 1,2-dioleoyl-*sn*-glycero-3-(phospho-L-serine); egg PC, egg phosphatidylcholine; egg PG, egg phosphatidylglycerol; EM, electron microscopy; FITC-dextran, fluorescein isothiocyanate conjugated to dextran; HBS, HEPES-buffered saline; LB, Lewy body; MW, molecular mass; Mon, monomer; PD, Parkinson's disease; PF, protofibril; POPE, 1-palmitoyl-2-oleoyl-*sn*-glycero-3-phosphoethanolamine; POPG, 1-palmitoyl-2-oleoyl-*sn*-glycero-3-[phospho-*rac*-(1-glycerol)]; RT, room temperature; wt, human wild type.

10.1021/bi0121353 CCC: $22.00
Published on Web 03/15/2002

This paper represents a continuation and expansion of our previous vesicle permeabilization studies (*12*), focusing on the membrane permeabilizing activities of the monomeric and protofibrillar states of α-synuclein under various conditions, and on the effects of the PD-linked mutations. The data below address the mechanism of permeabilization in our model systems, and the specific activities of the mutant, wt, and mouse forms of α-synuclein. These findings have implications for our understanding of the protofibril as a potentially pathogenic species in Parkinson's disease.

EXPERIMENTAL PROCEDURES

Protofibril and Monomer Purification. Recombinant α-synucleins were expressed in *Escherichia coli* and purified essentially as described by Conway et al. (*20*), at the Center for Biocatalysis and Bioprocessing at the University of Iowa (Iowa City, IA). Protofibrillar α-synuclein was prepared and purified as previously described (*12*). Briefly, lyophilized α-synuclein was dissolved at a concentration of 1−2 mM in 10 mM potassium phosphate and 140 mM NaCl (pH 7.4) on ice over a period of approximately 30 min. The solution was filtered [0.22 μm nylon Spin-X (Corning Costar)], injected onto a Superdex 200 (HR 10/30) column, and eluted with HBS [10 mM HEPES and 145 mM KCl (pH 7.4)] at 0.5 mL/min while monitoring UV absorbance at 280 nm. Protofibril and monomeric fractions of α-synuclein were collected, and the protofibril fraction was concentrated 3−4-fold using either Microcon 100 kDa or Ultrafree (5−50 kDa cutoff was suitable) centrifugal concentrators (Millipore). Protofibril fractions prepared using this method (*12*) are heterogeneous and contain structures (by AFM, EM, and gel filtration) similar to protofibril fractions evolved over longer time periods, as in refs *5* and *7*. Protofibril fractions were stored at 4 °C and generally used within a few days. Control experiments showed that the concentration device itself did not influence protofibril activity. Protein concentrations were determined by quantitative amino acids analysis.

Phospholipid Vesicle Preparation. All lipids were obtained from Avanti Polar Lipids except cholesterol (Sigma). Vesicles were prepared by membrane extrusion (*21*, *22*). Lipids were dissolved in chloroform (approximately 20 mg/mL, 1 mL total) and dried onto the surface of a 25 mL round-bottom flask using a rotary evaporator and, subsequently, a lyophilizer. Lipid mixtures (1:1 mass/mass ratio except for the cholesterol/lipid mixture, which had a 2:1 ratio) were dissolved together in chloroform before drying. Dried lipids were resuspended at 20 mg/mL in HBS, 1 mM EDTA, 100 mg of 1 mm diameter glass beads, and either fura-2 (100 μM, Molecular Probes), cytochrome *c* (300 μM, Sigma, from horse heart), or FITC-dextran 4000 (62 μM, average MW of 4400, Sigma FD-4). Vesicles were also prepared that contained dopamine [50 mM unlabeled dopamine with 10 μCi of [2,5,6-^{3}H]dopamine (Amersham)], and in this case, the buffer was 10 mM CH_3COOH, 145 mM KCl, and 1 mM EDTA (pH 5.1). The vesicle suspension was rotated (rotary evaporator, ∼75 rpm) at room temperature and pressure for 30 min, and then allowed to incubate without rotation for 2 h. The vesicles were then extruded (Avanti Mini-Extruder) through a 100 nm filter (Whatman Nuclepore) 11 times and then through a second 100 nm filter 11 times. Vesicles and their contents were purified from free material into HBS and 1 mM EDTA using either a PD-10 (fura-2 and dopamine) or a Superose 12 (cytC and FITC-dextran; HR 10/30, 0.5 mL/min) size exclusion column, and stored in glass vials at 4 °C in the dark. Dopamine-containing vesicles were used within 24 h due to the high background leakage rate of dopamine. The mean vesicle diameter was confirmed to be slightly larger than 100 nm by negative stain EM (*12*). The phospholipid content was determined using the Bartlett assay (*23*) as modified by New (*22*).

Conditions for Membrane Permeability Measurement. Vesicles were diluted 10-fold in HBS and mixed with an equal volume of sample in HBS (with or without 10 mM $CaCl_2$ as indicated; final phospholipid concentration of approximately 0.65 mM). The solution was incubated at RT for 30 min in darkness, and then assayed for inward calcium leakage or outward flux of entrapped contents, as described below. Data are expressed as a fraction of the maximum effect (ionomycin or Triton X-100; see below): (measured signal − blank signal)/(maximum signal − blank signal). Because it was not desirable to wait for protofibril concentration results from amino acids analysis, concentrations were not exactly matched. A small dilution series was generally performed in each experiment (the scattering contribution to UV absorbance and the detergent/denaturant resistance of protofibrils precluded using a more traditional protein assay). After the protein concentration results had been received, approximately matched concentrations from the dilution series were chosen; the observed concentration dependences (i.e., Figure 1 and ref *12*) were not steep enough that this influenced our conclusions.

Measurement of the Extent of Inward Calcium Leakage. Following the incubation, samples (generally 10 μL) were injected directly through a Kratos HPLC fluorescence detector (see ref *12* for further details) using either a syringe pump (PHD 2000, Harvard Apparatus) with a 9725i Rheodyne injector or a Waters 2690 HPLC system (0.5 mL/min HBS, 5 mM $CaCl_2$). Data from the detector were digitized at 10 Hz (Waters SAT/IN module). The total signal was determined by integration of the peak area in the chromatogram using Waters Millenium32 software. Ionomycin (Sigma, 31 nM) was used as a positive control for maximum signal. Melittin, from bee venom, was purchased from Sigma. Control experiments using vesicles not containing fura-2 showed that an insignificant portion of the fluorescence signal was due to light scattering.

Measurement of the Extent of Vesicular Content Leakage. Vesicle incubations were ultrafiltered (Microcon 100 device, 12000*g*, 3 min) to separate vesicles and entrapped materials from compounds free in solution. Filters were prewashed with 60 μL of HBS (12000*g*, 4 min) to reduce background fluorescence and absorbance from the filters. Triton X-100 (0.5% final concentration) was used as a positive control; each entrapped compound used in this study, after its release from the vesicle, passed quantitatively through the 100 kDa filter, and it was verified that the relevant spectral properties were not altered by the presence of Triton X-100. Filtrate was analyzed as described above by injection through the appropriate detector (0.5 mL/min HBS): cytC, absorbance at 410 nm (Waters 996 PDA); FITC-dextran, Waters 474 fluorescence detector, excitation at 490 nm with a bandwidth of 18 nm, emission at 520 nm with a bandwidth of 10 nm; fura-2, Kratos fluorescence detector, optical details as in

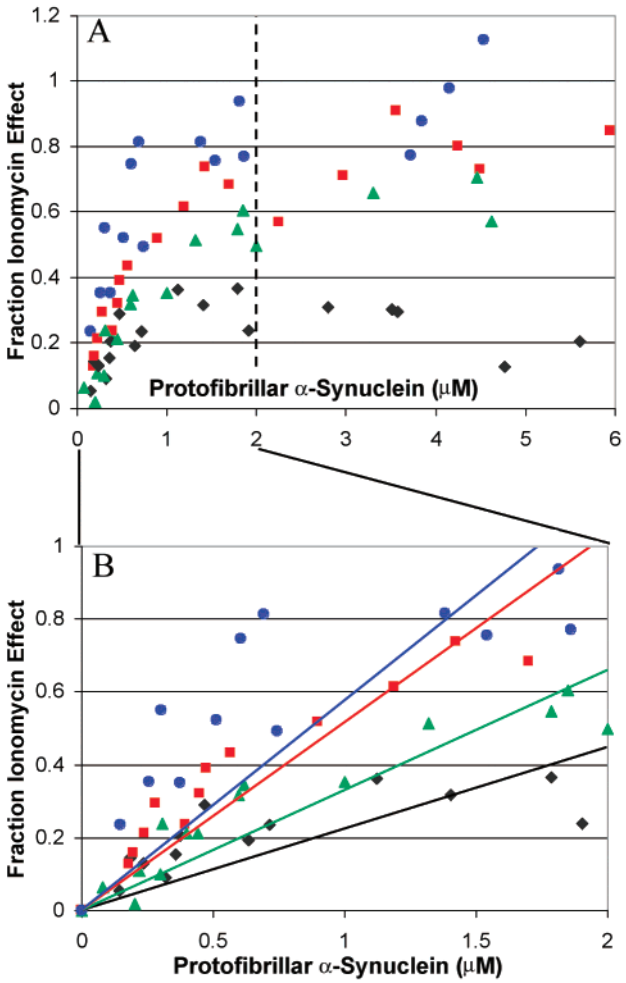

FIGURE 1: Concentration dependence of egg PG vesicle permeabilization to calcium by protofibrils of α-synuclein. Data shown are from wt (black diamonds), A30P (green triangles), A53T (blue circles), and mouse (red squares) protofibrillar α-synuclein. Protein and vesicles were incubated for 30 min in the presence of 5 mM $CaCl_2$ followed by a fura-2 fluorescence measurement. The protofibril population is a heterogeneous mixture of oligomeric species; protein concentrations are given in terms of monomeric α-synuclein, as discussed in the text. (A) The dashed line approximately separates the concentration-independent portion of the curve from the concentration-dependent region. The data from the concentration-dependent region (0−2 μM) are also shown in panel B on an expanded *x*-axis. Each line represents a linear least-squares fit to the data in this range.

ref *12*. In the case of fura-2 leakage experiments without calcium, $CaCl_2$ was added to the filtrate (to a final concentration of 5 mM) before analysis to saturate fura-2, and the mobile phase was HBS with 5 mM $CaCl_2$. Tritiated dopamine filtrate was counted to 2% precision using a Beckman LS6500 liquid scintillation counter (Fisher Scintisafe 30% scintillant; all samples exhibited identical levels of quenching by the channels ratio method).

Light Scattering. Incubations were performed as described above, with subsequent injection of the sample through a Waters 474 fluorescence detector (excitation at 600 nm with a bandwidth of 18 nm, emission at 600 nm with a bandwidth of 10 nm), using a mobile phase of 0.5 mL/min HBS or HBS with 5 mM $CaCl_2$. As a control, after Triton X-100 (0.5%) solubilization of the vesicles, almost no light scattering signal was seen; protofibrils and monomer alone (without vesicles) also gave almost no signal. Blank incubations of vesicles with and without 5 mM $CaCl_2$ showed no significant differences in light scattering.

Vesicle Fusion Measurements. Fluorescently labeled vesicles (egg PG with 1 mol % each NBD-DPPE and lissamine rhodamine B-DPPE, both headgroup-labeled) were prepared exactly as described above (20 mg of lipid, dispersed in 1 mL of HBS with 1 mM EDTA, extrusion through 100 nm membranes, PD-10 chromatography). The labeled vesicles were diluted 10-fold with a stock of unlabeled egg PG vesicles. This mixture was subsequently diluted 10-fold in HBS and mixed (1:1) with a sample (with or without 10 mM $CaCl_2$). Samples containing calcium were incubated for 30 min at RT; samples not containing calcium were incubated for 20 min at RT followed by dilution (1:1) into HBS with 5 mM $CaCl_2$ (to obtain a final calcium concentration consistent with the incubations containing calcium) and incubation for a further 10 min. The amount of resonance energy transfer from NBD to rhodamine (by NBD emission) was measured using a fluorescence detector (*24*) (Waters 474, excitation at 455 nm with a bandwidth of 18 nm, emission at 530 nm with a bandwidth of 10 nm, 0.5 mL/min HBS with 5 mM $CaCl_2$). Positive controls, lipid dilution with Triton X-100 (0.5%) or fusion using high concentrations of $CaCl_2$ (20 mM), gave several-fold increases in signal.

RESULTS

Protofibrils Comprising Parkinson's Disease-Linked Variants Have a Higher Specific Vesicle Permeabilizing Activity Than Those Composed of the wt Protein. Purified protofibrillar α-synuclein at various concentrations (based on the total number of moles of protein) was incubated for 30 min with egg PG vesicles containing the dye fura-2, followed by fluorescence measurements of the calcium/fura-2 chelate (Figure 1). Note that although increased fluorescence can result from calcium leakage inward or fura-2 leakage outward, the latter process contributes only a relatively small amount to the signal (see below, Figure 2, and ref *12*). The permeabilization reaction initially proceeds via a fast phase followed by a slower increase in signal, much of which is due to background calcium leakage (ref *12* and unpublished results). Measurement at 30 min was chosen because this point lies near the end of the initial fast phase. α-Synuclein protofibrils comprising A53T (Figure 1A, blue), mouse (red), and A30P (green) are each significantly stronger permeabilizers than the wt protein (black). Mouse, A30P, and A53T α-synucleins, like wt (*12*), exhibited a concentration dependence up to ~2 μM (Figure 1B).

To rule out instability of protofibrils as a factor influencing the results presented above, experiments were performed in which protofibrils were rechromatographed immediately following the permeabilization assay. In every case, we found <10% dissociation to monomer (by 280 nm absorbance) and the amount of dissociation did not correlate with permeabilizing activity. At a significantly higher protein concentration (23 μM), monomeric α-synuclein (wt, A30P, A53T, and mouse) caused ≤15% of the ionomycin effect, using egg PG or POPG vesicles (data not shown).

Statistically significant differences between A53T, A30P, and wt could not be observed using our previous conditions (*12*). To reduce experimental error, uniform protein purifications (all synucleins in this study were produced and purified by the Center for Biocatalysis and Bioprocessing at the

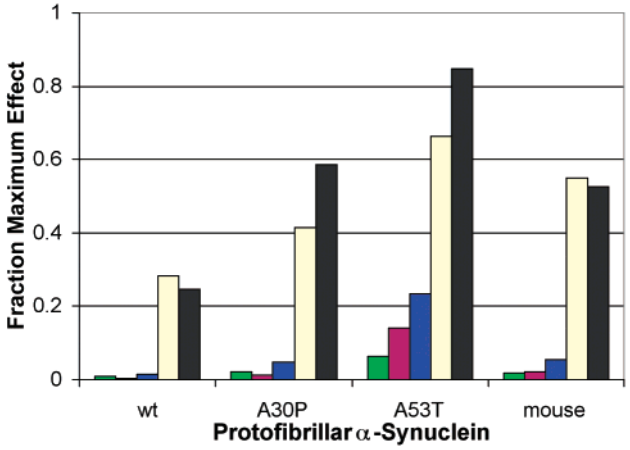

FIGURE 2: Size dependence of the leakage of molecules across PG vesicle membranes induced by protofibrillar α-synuclein during a 30 min incubation in the presence of 5 mM $CaCl_2$. Representative data are shown for cytochrome *c* (green bars, POPG vesicles), FITC-dextran 4000 (maroon bars, POPG), fura-2 (blue bars, POPG; egg PG gave identical results), dopamine (yellow bars, egg PG), and calcium (black bars, POPG). The protein concentrations were (in the order wt, A30P, A53T, and mouse, for each type of experiment): 9.5, 8.9, 7.7, and 6.0 μM (cytC and dextran); 6.0, 7.4, 7.5, and 10.2 μM (fura-2); 4.6, 5.0, 3.8, and 4.2 μM (dopamine); 4.6, 5.0, 7.5, and 4.2 μM (calcium). These concentrations are in excess of the value at which the concentration dependence essentially disappears (Figure 1 and ref *12*).

University of Iowa) and highly unilamellar vesicle preparations (the protofibril cannot permeabilize the inner chambers of a multilamellar vesicle) were used. Elimination of methanol from the lipid solutions may have produced more uniform unilamellar preparations.

Protofibril-Induced Permeabilization of Vesicular Membranes Is Strongly Size-Selective in the Presence of Calcium. Figure 2 shows the extent of leakage of molecules of cytochrome *c* (green; MW = 12 384 Da), FITC-dextran (maroon; MW = 4400 Da), fura-2 (blue; MW = 832 Da), dopamine (yellow; MW = 189.6 Da), and calcium (black). While one must be cautious in interpreting the results quantitatively,[2] there is clearly a strong inverse correlation between molecular mass and extent of leakage. A53T consistently (in six out of six experiments using either dextran or fura-2 vesicles) showed a greater degree of permeabilization to larger molecules than the other variants (albeit still to a small extent), suggesting that the A53T permeabilizing structures may be intrinsically different from the other variants. No permeabilization to cytC, dextran, or dopamine was induced by monomeric α-synuclein in the presence of calcium (data not shown).

Increased Leakage of Vesicular Contents Was Induced by Protofibrillar and, to a Lesser Extent, Monomeric α-Synuclein in the Absence of Calcium. In the absence of calcium (data not shown), protofibrils allow dopamine and even larger molecules that were mainly impermeant in the presence of calcium (Figure 2; cytC, dextran, and fura-2) to pass through the membrane (ca. 30% leakage, ~6 μM protein). Under these conditions, the wt protofibrils were less efficacious in causing permeabilization of these larger molecules than the other three variants.

[2] Important considerations include calcium chelation by EDTA within the vesicles, the net charge of the permeating species, and cytC−vesicle interactions (*25*).

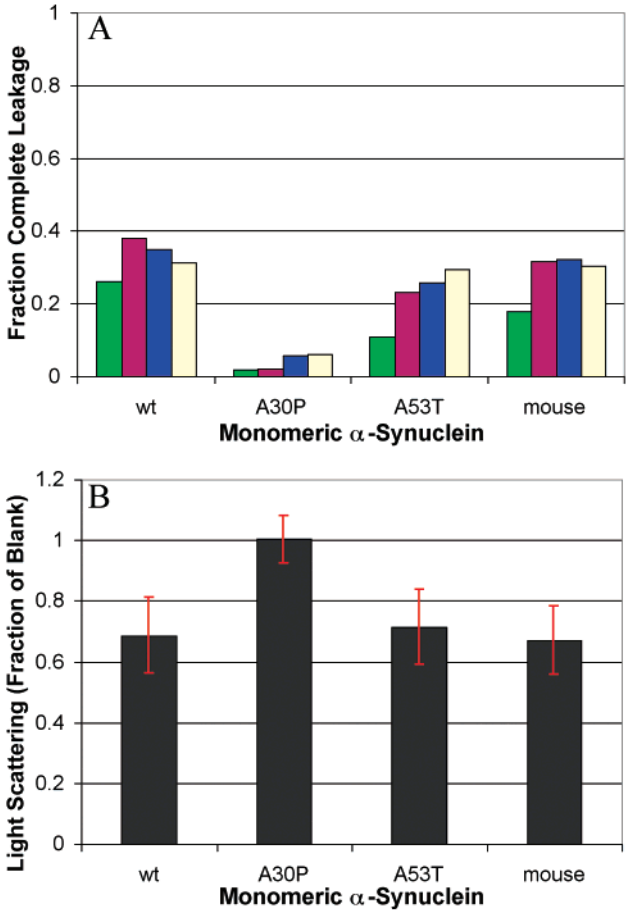

FIGURE 3: Leakage of molecules across destabilized (no calcium) PG vesicle membranes and changes in vesicular light scattering induced by four variants of the α-synuclein monomer (23 μM). (A) Representative permeabilization data are shown for cytochrome *c* (green bars, POPG vesicles), FITC-dextran 4000 (maroon bars, POPG), fura-2 (blue bars, POPG), and dopamine (yellow bars, egg PG). (B) Light scattering data values are given as the ratio of 90° scattering intensity (600 nm) in the sample to the intensity from a blank containing vesicles but no protein. The experiments gave identical results with both egg PG and POPG vesicles; data from both sets were therefore averaged and shown. Error bars are ±one SD in height.

Similar experiments performed with monomers in the absence of calcium, at the comparable concentration of 8 μM, showed little permeabilization to any of the molecules (cytC, dextran, fura-2, and dopamine; fraction of leakage of <0.1 on average; data not shown). However, at much higher concentrations (23 μM), three of the α-synuclein monomer variants, wt, A53T, and mouse, caused leakage (without obvious size selectivity) from vesicles (Figure 3A). Monomeric A30P, however, had almost no activity in permeabilizing these vesicles.

Monomeric α-Synuclein, at High Concentrations, Exhibits Detergent-like Properties. Figure 3B shows that monomeric A53T, wt, and mouse α-synuclein at high concentration (23 μM) induce a detergent-like effect on calcium-free vesicles, as evidenced by decreased light scattering, which suggests vesicle lysis. The exception is A30P, the only variant which did not permeabilize vesicles (Figure 3A). A detergent mechanism of permeabilization by monomeric synuclein would not be expected to show a size selectivity for permeating molecules (*26*), which is exactly what was observed (Figure 3A).

Permeabilization Is Not Accompanied by Significant Vesicle Aggregation or Fusion. Light scattering experiments using the vesicle incubations described above were performed to test the possibility that vesicle aggregation and/or fusion was induced by protofibrillar α-synuclein. Protofibrillar α-synuclein caused an increase in vesicular light scattering of less than 1.7-fold in the absence of calcium (egg PG or POPG; data not shown). Similarly, both protofibrillar and monomeric α-synuclein (wt, A30P, A53T, and mouse of each) caused increases in light scattering of <1.5-fold in the presence of 5 mM $CaCl_2$ (egg PG vesicles; data not shown). Changes of this magnitude can be ascribed to protein−vesicle binding, whereas fusion or large-scale aggregation generally gives a many-fold increase in light scattering (*27*). One caveat to this experiment is that a small amount of α-synuclein-induced vesicle solubilization (lysis) in combination with the background light scattering increase due to protein−vesicle binding might not be observed.

To conclusively rule out the occurrence of vesicle fusion, we carried out a standard vesicle fusion assay based on FRET between NBD and rhodamine-labeled lipids (*24*). Under each of the conditions that was tested (with and without calcium; monomer and protofibril of each α-synuclein variant), no vesicle fusion was detected (data not shown).

Effects of Vesicle Composition on Permeabilization. α-Synuclein is known to bind to acidic and 50 mol % acidic (1:1 PC or PE with PA, PS, or PI), but not neutral vesicles in both its monomeric (*12*, *15*) and protofibrillar (*12*) forms. One report has stated that 50 mol % PE in otherwise acidic vesicles increased the level of monomer binding relative to 50 mol % PC (*14*). We examined protofibril-induced permeabilization of vesicles composed of mixtures of PG and neutral lipids (PC, PE, or cholesterol) in a 1:1 molar ratio. These three types of 50% neutral vesicles were not permeabilizable to calcium (5 mM) by protofibrils (∼11 μM; data not shown).

The phase transition temperatures for POPG and egg PG are −2 °C and approximately −10 °C, respectively. When one considers that our experiments were performed at RT, it is unlikely that an isothermal phase transition played a role in the permeabilization mechanism. Additionally, the results of calcium permeabilization experiments (using monomeric or protofibrillar α-synuclein) were similar when either DOPG (transition temperature of −18 °C) or POPG (Figure 2) vesicles were used, ruling out a phase transition as a mechanism for permeabilization (data not shown).

Figure 4 shows the results of permeabilization of vesicles composed of other (non-PG) negatively charged lipid headgroups. These experiments were performed in the absence of calcium, since calcium (5 mM) produced flocculation of DOPA and DOPS membranes, which are more sensitive to calcium aggregation/fusion than PG vesicles (*28*). DOPG was included as a control, and was permeabilized by protofibrillar and, to a lesser extent, monomeric (at a relatively high protein concentration) α-synuclein. DOPS, however, was resistant to protofibril and monomer permeabilization. On the other hand, DOPA was permeabilized by the A53T protofibril (though not monomer), similar to PG in the presence of calcium. It is unlikely that either DOPS or DOPA (transition temperature of −11 or −8 °C, respectively) undergoes an α-synuclein-induced phase transition under these conditions.

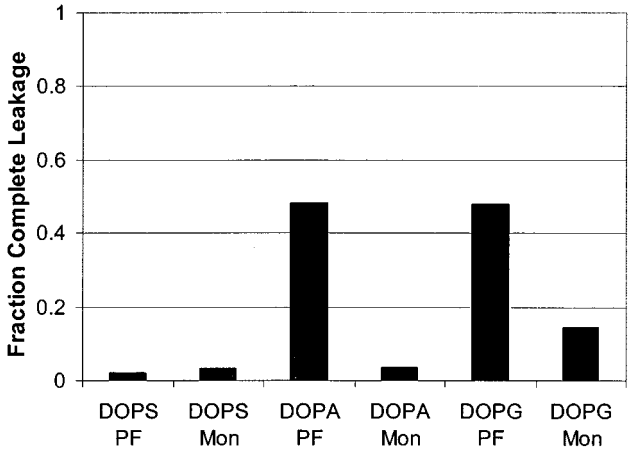

FIGURE 4: Permeabilization of vesicles composed of non-PG lipids. Leakage of fura-2 (representative data) from vesicles composed of lipids with various negatively charged headgroups by protofibrillar (PF) (9.7 μM) and monomeric (Mon) (35.5 μM) A53T α-synuclein. The solutions in these experiments did not contain $CaCl_2$.

Monomeric α-Synuclein Can Suppress Protofibril Permeabilization. Monomeric α-synuclein can interfere with the protofibril-specific permeabilization process (Figure 5, first six bars). Both wt and A30P monomer can reduce the extent of permeabilization by protofibrils comprising either variant. It is probable that inhibition occurs through monomer binding to vesicles, which would decrease surface charge density on the membrane, thereby decreasing protofibril binding affinity and/or strengthening the membrane against protofibril attack (similar to the calcium effect). Alternatively, monomeric α-synuclein could inhibit protofibril binding by simple steric blockage of the membrane surface. While either one of these mechanisms or a combination is probable, we cannot rule out an inhibitory mechanism in which monomer binds to the protofibril directly.

To test for the generality of this inhibition process, we used another known vesicle permeabilizer, melittin. In this case, we observed that melittin permeabilization was enhanced by either A30P or wt monomeric α-synuclein (Figure 5, last three bars; 5 mM $CaCl_2$). As discussed above, the monomer alone does not cause significant permeabilization under these conditions. Melittin permeabilization (but not binding) is inhibited by the presence of negatively charged lipids (*29*). Decreased membrane surface charge and membrane destabilization due to bound monomeric α-synuclein are therefore potential mechanisms of enhancement.

DISCUSSION

α-Synuclein is linked to early-onset Parkinson's disease by two point mutations, A53T and A30P (*2*, *3*). Examining the biophysical differences between these mutants and the wt protein is one approach to gaining an understanding of PD pathogenesis. α-Synuclein is known to bind negatively charged membranes in its monomeric and, to a much greater extent, its protofibrillar states (*12*−*15*). However, only the protofibrillar form permeabilizes vesicles in the presence of calcium (*12*). The wt, A53T, and A30P protofibrils exhibit pore-like structural properties (*5*, *12*; H. Lashuel and P. T. Lansbury, Jr., unpublished data; T. Ding and P. T. Lansbury, Jr., unpublished data).

Protofibril Permeabilization Mechanism. Protofibrillar α-synuclein exhibits a strong size selectivity in allowing

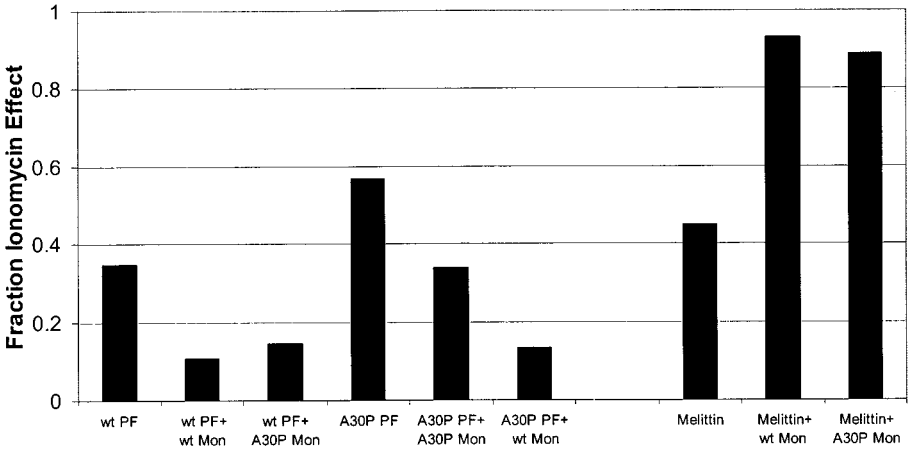

FIGURE 5: Monomeric α-synuclein can suppress or enhance permeabilization to calcium induced by protofibrils or melittin, respectively. Samples were prepared in 10 mM $CaCl_2$, mixed 1:1 with a vesicle solution, and incubated for 30 min, and then fura-2 fluorescence was measured. For the left six bars, wt and A30P monomer (Mon) (11.5 μM) can suppress permeabilization of POPG vesicles induced by protofibrillar (PF) α-synuclein (wt, 3.0 μM; A30P, 3.7 μM). For the right three bars, permeabilization of egg PG vesicles by melittin (0.8 μM) is enhanced by co-incubation with wt or A30P monomeric α-synucleins (11 μM).

molecules to permeate PG vesicles (Figure 2). This property suggests that protofibrillar α-synuclein permeabilizes in a pore-like fashion. On the basis of the impermeability of FITC-dextran [MW = 4400 Da; prolate ellipsoidal in shape with a small axis diameter of 26 Å (*30*)], we conclude that the protofibril "pore" must have an inner diameter of less than approximately 25 Å. This diameter is consistent with annular structures observed by EM (H. Lashuel and P. T. Lansbury, Jr., unpublished data).

The protofibril concentrations reported in this study are given in terms of monomeric α-synuclein. The actual concentration of protofibrils will be many-fold lower, because numerous α-synuclein monomers combine to form a single protofibril. While "protofibril" refers to a heterogeneous pool of species (the distribution of which may depend on the variant), a typical protofibril may contain on the order of 20 monomers, as estimated from dimensions measured by AFM (T. Ding and P. T. Lansbury, Jr., unpublished data).

Permeabilization by High Monomer Concentrations. Monomeric α-synuclein is capable of permeabilizing only relatively unstable vesicles by a detergent-like mechanism, and only at relatively high concentrations (Figure 3). Interestingly, A30P does not have this property, which may be due to the proline at position 30 interfering with N-terminal helix formation (*18*) which is concomitant with binding (*13*). α-Synuclein of undetermined aggregation state had a disruptive effect on planar supported lipid bilayers of PC and PS (1:1) (*14*). The mechanism underlying that observation may be similar to the detergent-like solubilization described here.

Effects of Calcium on the Model System. Calcium has strong modulating effects on our in vitro permeabilization system. Calcium is known to affect the structure and properties of PG membranes in several ways: (i) increased phase transition temperature at low concentrations (*28*, *31*); (ii) increased levels of aggregation, fusion, and cochleate cylinder formation at high concentrations (*31*, *32*); and (iii) membrane condensation (decreased area per lipid molecule) and decreased ionic permeability (*32*, *33*). As discussed above, we have ruled out a phase transition as a likely permeabilization mechanism, and calcium did not cause significant aggregation or fusion. Therefore, the effects of calcium observed in this study may be due to calcium binding by the vesicles, reducing electrostatic surface charge density, and causing membrane condensation. Membrane condensation could decrease the level of permeabilization by increasing the amount of energy required for protein insertion into the bilayer and/or the amount of energy required for bilayer disruption. A change in the balance between these two effects could at least in part be responsible for the change in size selectivity of protofibril-induced permeability as a function of calcium. A reduction in surface electrostatic charge density could likewise alter the binding affinity and/or insertion/disruption energy of α-synuclein. An alternative possibility which could explain the modulating effects of calcium is a direct calcium−protein interaction (*34*). A diminished level of permeabilization of POPG membranes to the fluorophores ANTS/DPX by millimolar levels of calcium has been observed previously in the case of the HIV-1 fusion peptide (*35*).

Stoichiometry of Membrane Permeabilization by Protofibrillar α-Synuclein. Consideration of the approximate stoichiometries of binding can also give insights into the mechanism. A typical phospholipid concentration in an experiment reported here is 0.65 mM. Using an equation relating vesicle size to phospholipid number (*36*), it can be calculated that a 1500 Å diameter vesicle contains ~200000 lipid molecules, with a surface area of 7×10^6 Å^2. Therefore, the typical vesicle concentration in an experiment is 3 nM. Using an experimental estimate of 20 monomers/protofibril from AFM, our experiments are typically done with protofibril concentrations of 25 nM to several hundred nanomolar. Furthermore, the surface area of a vesicle could accommodate approximately 400 protofibrils.[3] Calcium permeabilization was still clearly detected at approximately 25 nM (protofibril concentration), or an average of eight protofibrils (160 α-synuclein molecules) per vesicle (Figure 1). These rough

[3] A protofibril can be reasonably modeled as a 150 Å diameter sphere (based on structures observed by AFM). A great circle of this sphere (obtained by intersection with a plane through the center of the sphere) has an area of 18 000 Å^2. Dividing the total vesicular surface area by this value gives an upper limit to the number of protofibrils which can fit onto one vesicle, since this calculation ignores packing considerations on the vesicular surface.

calculations demonstrate that complete coating of the vesicle is not required for permeabilization, and further emphasize that leakage under these conditions probably occurs via a localized, pore-like mechanism. Meanwhile, monomeric α-synuclein at more than 7000 molecules per vesicle does not permeabilize the membranes to calcium (discussed above).

Relevance to Parkinson's Disease. The finding that membrane permeabilization depends on aggregation state (Figure 1) is correlated with the fact that a major neuropathological feature of PD brain is the presence of aberrant α-synuclein secondary and quaternary structure. Our observation that the two PD-linked mutants of α-synuclein have greater specific permeabilizing activities than the wt protein (Figure 1) is consistent with membrane permeabilization being one pathogenic activity of the α-synuclein protofibril. Differences between the specific permeabilizing activities of the variants could arise from differences in the populations of various protofibril species and/or intrinsic differences in protofibril structure. However, specific activity is only one component of the critical factor in PD, that is, *total* activity. Thus, the differences in specific activity may be amplified, since protofibrillar species are known to accumulate faster for the mutants than for wt (*5*, *6*). These results are consistent with membrane permeabilization being a potentially neurotoxic mechanism in PD, although there are several points to be kept in mind. The observed lack of permeabilization in 50% neutral membranes must be considered in relation to naturally occurring membranes, the phospholipids of which are generally <20% acidic. This preference for anionic vesicles is not unexpected, nor is it unprecedented. Rabbit neutrophil defensins permeabilize pure POPG vesicles, but not POPG vesicles with 50 mol % POPC or 35 mol % POPE (*37*). Although natural membrane toxins such as melittin permeabilize biological membranes immediately, and the biological consequences are immediate, Parkinson's disease is a chronic disease of the elderly, and a potentially pathologic mechanism need not be especially fast-acting or potent. Furthermore, the effective intracellular concentrations of protofibril may be higher than those used in this study, because of dopamine-induced protofibril accumulation (*11*) and cytoplasmic crowding effects (*38*, *39*). Additionally, transbilayer potential differences, such as those found in neuronal cells, could be important for inducing permeabilization. For example, the rabbit defensin neutrophil peptide 1 (*40*) and the antimicrobial peptide magainin I (*41*) both require a transmembrane potential for permeabilizing activity. Finally, lipid peroxidation, the level of which is increased in the *substantia nigra* of PD brain (*42*) and is known to cause changes in membrane permeability and fluidity (*42*), may predispose cellular membranes to permeabilization by protofibrillar α-synuclein. In summary, protofibril-induced membrane permeabilization could potentially be involved in the pathogenesis of PD, and further experiments are necessary to confirm that this mechanism is operative in vivo. We are currently studying permeabilization of various biological vesicles, including dopaminergic synaptic vesicles, to investigate this important question.

ACKNOWLEDGMENT

We thank Jean-Christophe Rochet (J.-C.R.) for many insightful discussions and June-Young Park for suggesting the experiments with monomer and protofibril mixtures. We also thank Ross Fredenburg and J.-C.R. for critical reading of the manuscript.

REFERENCES

1. Spillantini, M. G., Schmidt, M. L., Lee, V. M., Trojanowski, J. Q., Jakes, R., and Goedert, M. (1997) *Nature 388*, 839−840.
2. Kruger, R., Kuhn, W., Muller, T., Woitalla, D., Graeber, M., Kosel, S., Przuntek, H., Epplen, J. T., Schols, L., and Riess, O. (1998) *Nat. Genet. 18*, 106−108.
3. Polymeropoulos, M. H., Lavedan, C., Leroy, E., Ide, S. E., Dehejia, A., Dutra, A., Pike, B., Root, H., Rubenstein, J., Boyer, R., Stenroos, E. S., Chandrasekharappa, S., Athanassiadou, A., Papapetropoulos, T., Johnson, W. G., Lazzarini, A. M., Duvoisin, R. C., Di Iorio, G., Golbe, L. I., and Nussbaum, R. L. (1997) *Science 276*, 2045−2047.
4. Weinreb, P. H., Zhen, W., Poon, A. W., Conway, K. A., and Lansbury, P. T., Jr. (1996) *Biochemistry 35*, 13709−13715.
5. Conway, K. A., Lee, S. J., Rochet, J.-C., Ding, T. T., Williamson, R. E., and Lansbury, P. T., Jr. (2000) *Proc. Natl. Acad. Sci. U.S.A. 97*, 571−576.
6. Li, J., Uversky, V. N., and Fink, A. L. (2001) *Biochemistry 40*, 11604−11613.
7. Conway, K. A., Harper, J. D., and Lansbury, P. T., Jr. (1998) *Nat. Med. 4*, 1318−1320.
8. Narhi, L., Wood, S. J., Steavenson, S., Jiang, Y., Wu, G. M., Anafi, D., Kaufman, S. A., Martin, F., Sitney, K., Denis, P., Louis, J. C., Wypych, J., Biere, A. L., and Citron, M. (1999) *J. Biol. Chem. 274*, 9843−9846.
9. Rochet, J.-C., Conway, K. A., and Lansbury, P. T., Jr. (2000) *Biochemistry 39*, 10619−10626.
10. Masliah, E., Rockenstein, E., Veinbergs, I., Mallory, M., Hashimoto, M., Takeda, A., Sagara, Y., Sisk, A., and Mucke, L. (2000) *Science 287*, 1265−1269.
11. Conway, K. A., Rochet, J.-C., Bieganski, R. M., and Lansbury, P. T., Jr. (2001) *Science 294*, 1346−1349.
12. Volles, M. J., Lee, S. J., Rochet, J.-C., Shtilerman, M. D., Ding, T. T., Kessler, J. C., and Lansbury, P. T., Jr. (2001) *Biochemistry 40*, 7812−7819.
13. Perrin, R. J., Woods, W. S., Clayton, D. F., and George, J. M. (2000) *J. Biol. Chem. 275*, 34393−34398.
14. Jo, E., McLaurin, J., Yip, C. M., St George-Hyslop, P., and Fraser, P. E. (2000) *J. Biol. Chem. 275*, 34328−34334.
15. Davidson, W. S., Jonas, A., Clayton, D. F., and George, J. M. (1998) *J. Biol. Chem. 273*, 9443−9449.
16. Eliezer, D., Kutluay, E., Bussell, R., Jr., and Browne, G. (2001) *J. Mol. Biol. 307*, 1061−1073.
17. Jensen, P. H., Nielsen, M. S., Jakes, R., Dotti, C. G., and Goedert, M. (1998) *J. Biol. Chem. 273*, 26292−26294.
18. Bussell, R., Jr., and Eliezer, D. (2001) *J. Biol. Chem. 276*, 45996−46003.
19. Wallace, A. J., Stillman, T. J., Atkins, A., Jamieson, S. J., Bullough, P. A., Green, J., and Artymiuk, P. J. (2000) *Cell 100*, 265−276.
20. Conway, K. A., Harper, J. D., and Lansbury, P. T., Jr. (2000) *Biochemistry 39*, 2552−2563.
21. Olson, F., Hunt, C. A., Szoka, F. C., Vail, W. J., and Papahadjopoulos, D. (1979) *Biochim. Biophys. Acta 557*, 9−23.
22. New, R. R. C. (1990) *Liposomes: a practical approach*, IRL Press, Oxford, U.K.
23. Bartlett, G. M. (1959) *J. Biol. Chem. 234*, 466−468.
24. Struck, D. K., Hoekstra, D., and Pagano, R. E. (1981) *Biochemistry 20*, 4093−4099.
25. Subramanian, M., Jutila, A., and Kinnunen, P. K. (1998) *Biochemistry 37*, 1394−1402.
26. Parente, R. A., Nir, S., and Szoka, F. C., Jr. (1990) *Biochemistry 29*, 8720−8728.
27. Grant, E., Jr., Beeler, T. J., Taylor, K. M., Gable, K., and Roseman, M. A. (1992) *Biochemistry 31*, 9912−9918.
28. Papahadjopoulos, D., Vail, W. J., Pangborn, W. A., and Poste, G. (1976) *Biochim. Biophys. Acta 448*, 265−283.

29. Ladokhin, A. S., and White, S. H. (2001) *Biochim. Biophys. Acta 1514*, 253−260.
30. Wimley, W. C., Selsted, M. E., and White, S. H. (1994) *Protein Sci. 3*, 1362−1373.
31. Verkleij, A. J., de Kruyff, B., Ververgaert, P. H., Tocanne, J. F., and van Deenen, L. L. (1974) *Biochim. Biophys. Acta 339*, 432−437.
32. Tocanne, J. F., Ververgaert, P. H., Verkleij, A. J., and van Deenen, L. L. (1974) *Chem. Phys. Lipids 12*, 201−219.
33. Van Dijck, P. W., Ververgaert, P. H., Verkleij, A. J., van Deenen, L. L., and De Gier, J. (1975) *Biochim. Biophys. Acta 406*, 465−478.
34. Nielsen, M. S., Vorum, H., Lindersson, E., and Jensen, P. H. (2001) *J. Biol. Chem. 276*, 22680−22684.
35. Nieva, J. L., Nir, S., Muga, A., Goni, F. M., and Wilschut, J. (1994) *Biochemistry 33*, 3201−3209.
36. Weinstein, J. N., Yoshikami, S., Henkart, P., Blumenthal, R., and Hagins, W. A. (1977) *Science 195*, 489−492.
37. Hristova, K., Selsted, M. E., and White, S. H. (1996) *Biochemistry 35*, 11888−11894.
38. Shtilerman, M. D., Ding, T. T., and Lansbury, P. T., Jr. (2002) *Biochemistry 41*, 3855−3860.
39. Minton, A. P. (2000) *Curr. Opin. Struct. Biol. 10*, 34−39.
40. Kagan, B. L., Selsted, M. E., Ganz, T., and Lehrer, R. I. (1990) *Proc. Natl. Acad. Sci. U.S.A. 87*, 210−214.
41. Duclohier, H., Molle, G., and Spach, G. (1989) *Biophys. J. 56*, 1017−1021.
42. Farooqui, A. A., and Horrocks, L. A. (1998) *Cell. Mol. Neurobiol. 18*, 599−608.

BI0121353